*Supplementary Material*

# Multiple binding modes underlie cannabinoid recognition by peroxisome proliferator-activated receptor gamma

N. R. Carina Alves[1,2], Justina Miranda[1] and Lautaro D. Alvarez[1,2*]

[1]Departamento de Química Biológica, Facultad de Ciencias Exactas y Naturales, Universidad de Buenos Aires, Ciudad Universitaria, Buenos Aires C1428EGA, Argentina

[2]UMYMFOR, CONICET - Universidad de Buenos Aires, Ciudad Universitaria, Buenos Aires C1428EGA, Argentina

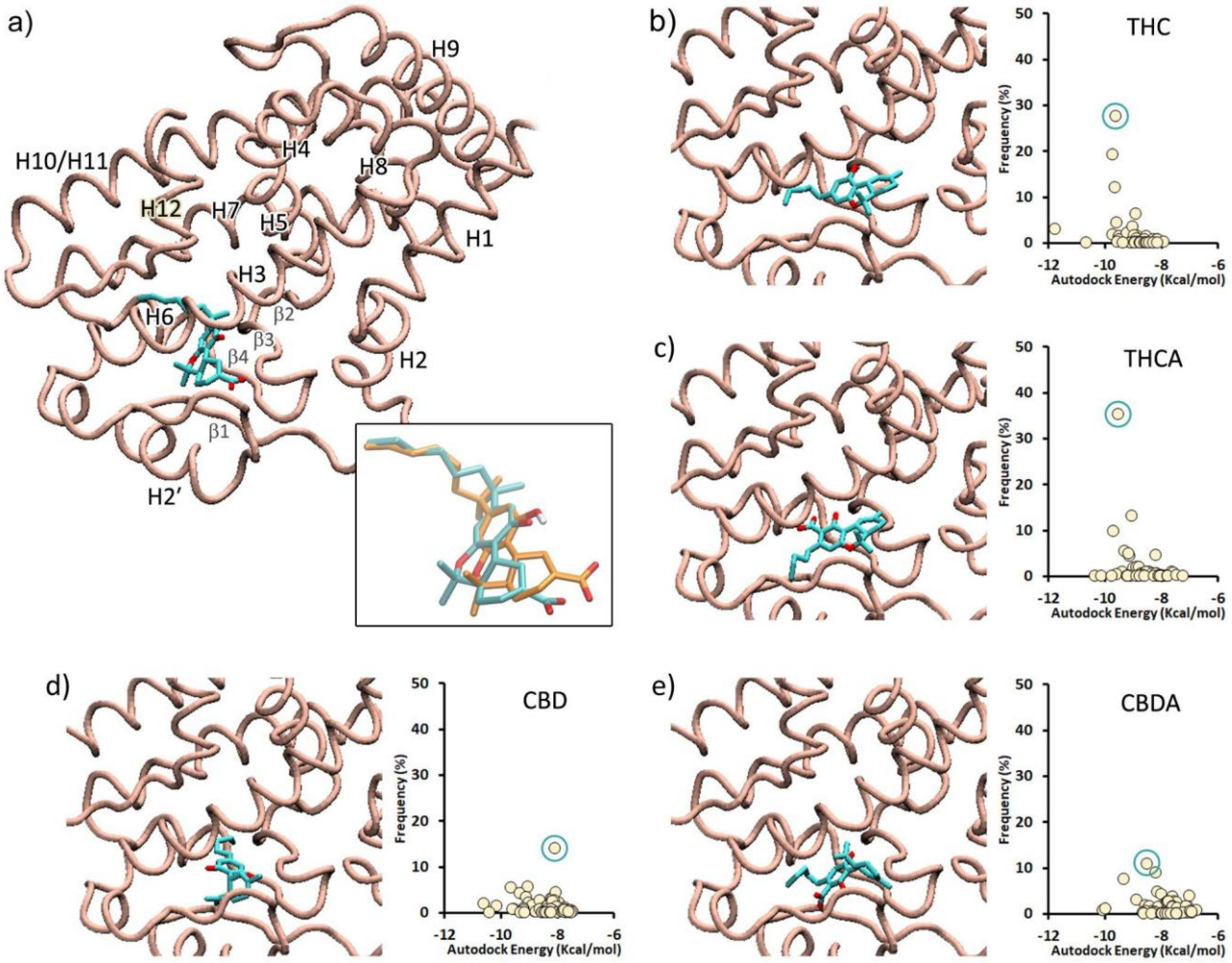


**Supplementary Figure S1.** (a) Crystal structure of the PPARγ LBD/AJA complex (PDB ID: 2OM9). Secondary structure elements are labeled. The inset shows the superposition of the crystallographic conformation (cyan carbon atoms) and the top-ranked redocked pose (orange carbon atoms) of AJA. The predicted binding energy was −9.7 Kcal/mol, and the corresponding docking cluster accounted for 67% of the generated poses. (b-e) Docking of cannabinoids into the PPARγ LBD/AJA structure (PDB ID: 2OM9). Left: lowest-energy solution from the most frequent cluster; right: Autodock4 frequencies and energies for THC (b), THCA (c), CBD (d), and CBDA (e).

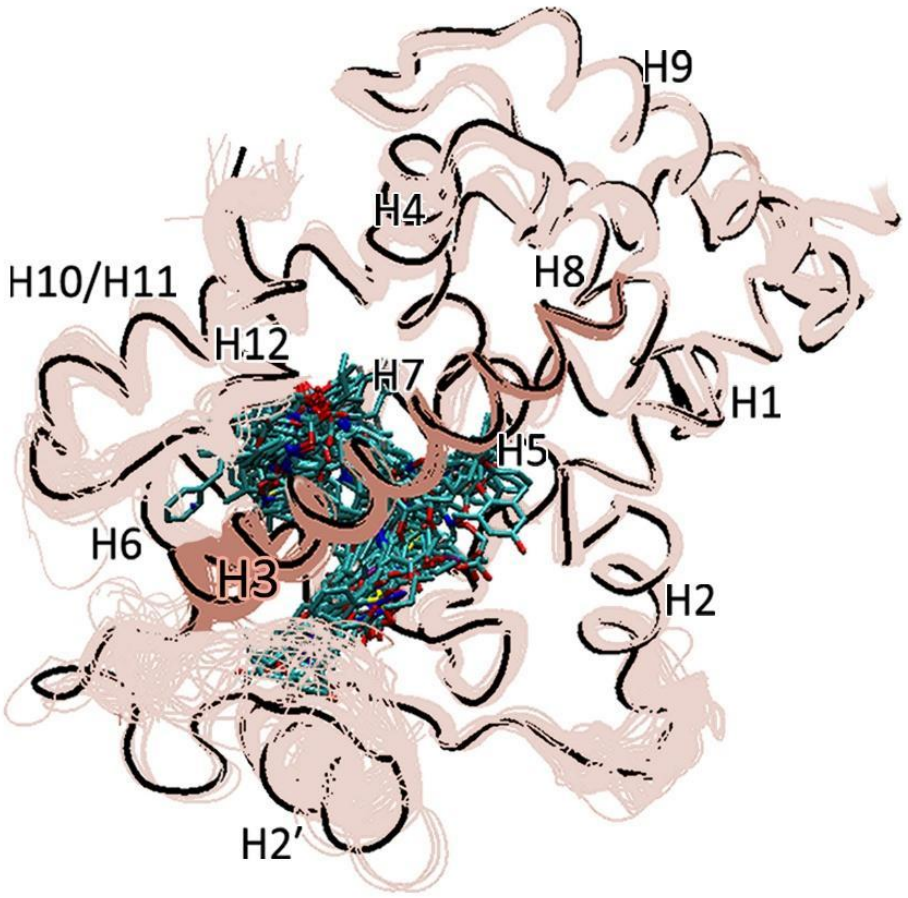


**Supplementary Figure S2.** Superposition of 70 PPARγ LBD-holo structures, showing the co-crystallized ligand in each case. The backbone of the PPARγ LBD-apo structure (PDB ID: 1PRG) is shown in black for reference.

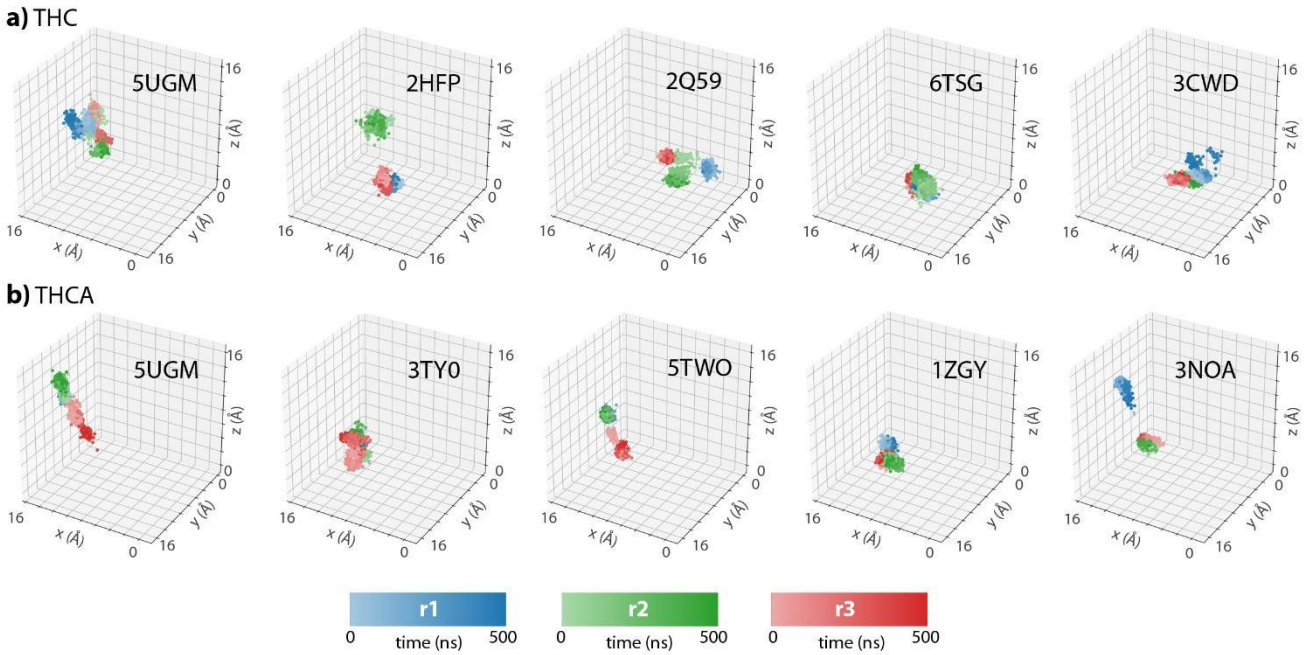


**Supplementary Figure S3.** Position of the ligand center of mass throughout the MD trajectories of PPARγ/THC (a) and PPARγ/THCA (b) complexes.

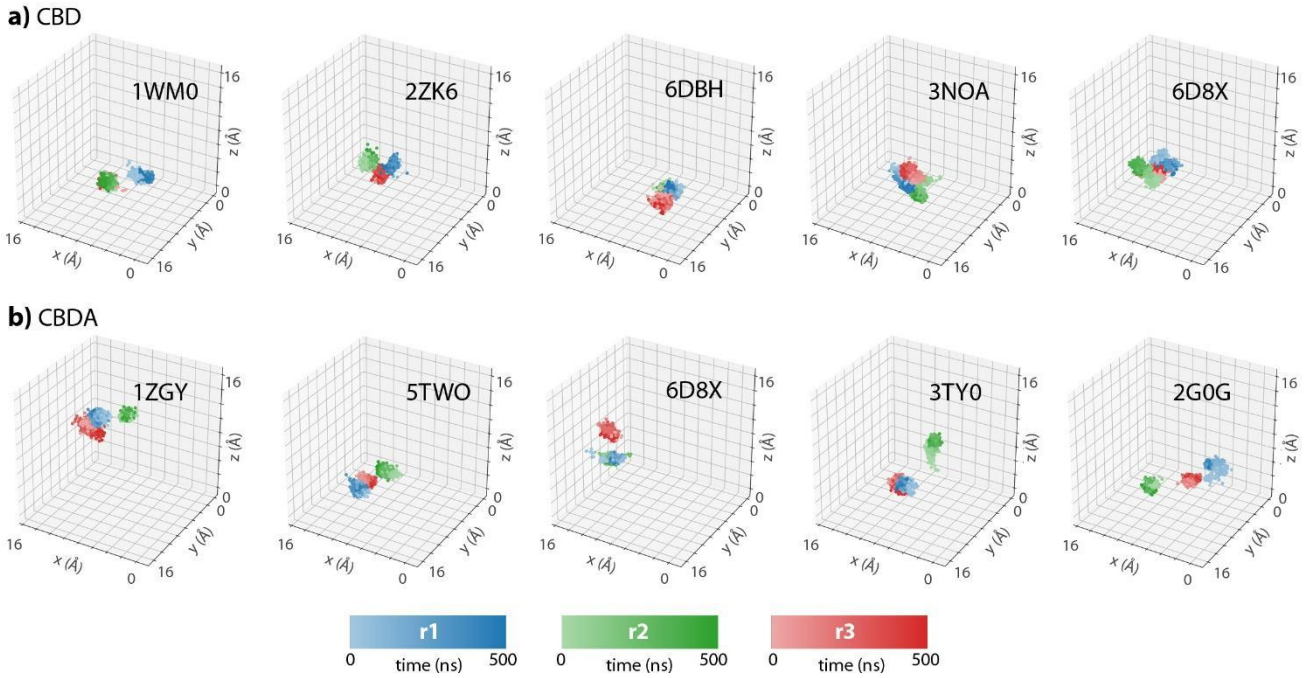


**Supplementary Figure S4.** Position of the ligand center of mass throughout the MD trajectories of PPARγ/CBD (a) and PPARγ/CBDA (b) complexes.

| | THC | | | | | | | | | | | | | | |
|---|---|---|---|---|---|---|---|---|---|---|---|---|---|---|---|
| | 5UGM | | | 2HFP | | | 2Q59 | | | 6TSG | | | 3CWD | | |
| | r1 | r2 | r3 | r1 | r2 | r3 | r1 | r2 | r3 | r1 | r2 | r3 | r1 | r2 | r3 |
| PCA variance | 0.73 | 0.83 | 1.10 | 0.08 | 0.24 | 0.92 | 0.10 | 0.97 | 0.07 | 0.45 | 0.89 | 0.23 | 2.54 | 0.27 | 0.17 |
| # Polar Interacions | 1 | 0 | 1 | 0 | 0 | 1 | 2 | 1 | 2 | 1 | 0 | 0 | 0 | 0 | 0 |
| # Aromatic Interactions | 0 | 0 | 0 | 1 | 0 | 0 | 2 | 1 | 2 | 0 | 0 | 0 | 0 | 0 | 0 |

| | THCA | | | | | | | | | | | | | | |
|---|---|---|---|---|---|---|---|---|---|---|---|---|---|---|---|
| | 5UGM | | | 3TYO | | | 5TWO | | | 1ZGY | | | 3NOA | | |
| | r1 | r2 | r3 | r1 | r2 | r3 | r1 | r2 | r3 | r1 | r2 | r3 | r1 | r2 | r3 |
| PCA variance | 0.22 | 0.31 | 1.03 | 0.10 | 1.31 | 0.82 | 0.12 | 0.20 | 0.66 | 0.14 | 0.24 | 0.12 | 0.20 | 0.12 | 0.23 |
| # Polar Interacions | 5 | 5 | 0 | 0 | 0 | 0 | 2 | 2 | 5 | 4 | 0 | 0 | 6 | 5 | 3 |
| # Aromatic Interactions | 0 | 0 | 0 | 0 | 0 | 0 | 0 | 0 | 0 | 0 | 0 | 0 | 0 | 0 | 0 |

| | CBD | | | | | | | | | | | | | | |
|---|---|---|---|---|---|---|---|---|---|---|---|---|---|---|---|
| | 1WM0 | | | 2ZK6 | | | 6DBH | | | 3NOA | | | 6D8X | | |
| | r1 | r2 | r3 | r1 | r2 | r3 | r1 | r2 | r3 | r1 | r2 | r3 | r1 | r2 | r3 |
| PCA variance | 0.62 | 0.18 | 0.18 | 0.11 | 0.42 | 0.20 | 0.17 | 0.10 | 0.36 | 0.45 | 0.74 | 0.60 | 0.52 | 0.78 | 0.44 |
| # Polar Interacions | 0 | 0 | 2 | 0 | 2 | 1 | 0 | 0 | 0 | 1 | 0 | 0 | 3 | 0 | 2 |
| # Aromatic Interactions | 0 | 0 | 0 | 0 | 0 | 0 | 0 | 0 | 0 | 2 | 0 | 0 | 1 | 0 | 0 |

| | CBDA | | | | | | | | | | | | | | |
|---|---|---|---|---|---|---|---|---|---|---|---|---|---|---|---|
| | 1ZGY | | | 5TWO | | | 6D8X | | | 3TY0 | | | 2G0G | | |
| | r1 | r2 | r3 | r1 | r2 | r3 | r1 | r2 | r3 | r1 | r2 | r3 | r1 | r2 | r3 |
| PCA variance | 0.17 | 0.08 | 0.28 | 0.13 | 0.23 | 0.27 | 0.17 | 0.30 | 0.23 | 0.10 | 0.32 | 0.12 | 0.28 | 0.19 | 0.52 |
| # Polar Interacions | 3 | 1 | 2 | 0 | 1 | 2 | 5 | 3 | 0 | 3 | 7 | 3 | 4 | 3 | 7 |
| # Aromatic Interactions | 0 | 1 | 0 | 0 | 0 | 0 | 1 | 1 | 0 | 0 | 0 | 0 | 2 | 1 | 0 |

**Supplementary Figure S5.** Variance of the PCA (PC1/PC2) projection, number of polar interactions, and number of aromatic-aromatic interactions with an occupancy greater than 40% along the simulation, for each of the simulated systems.

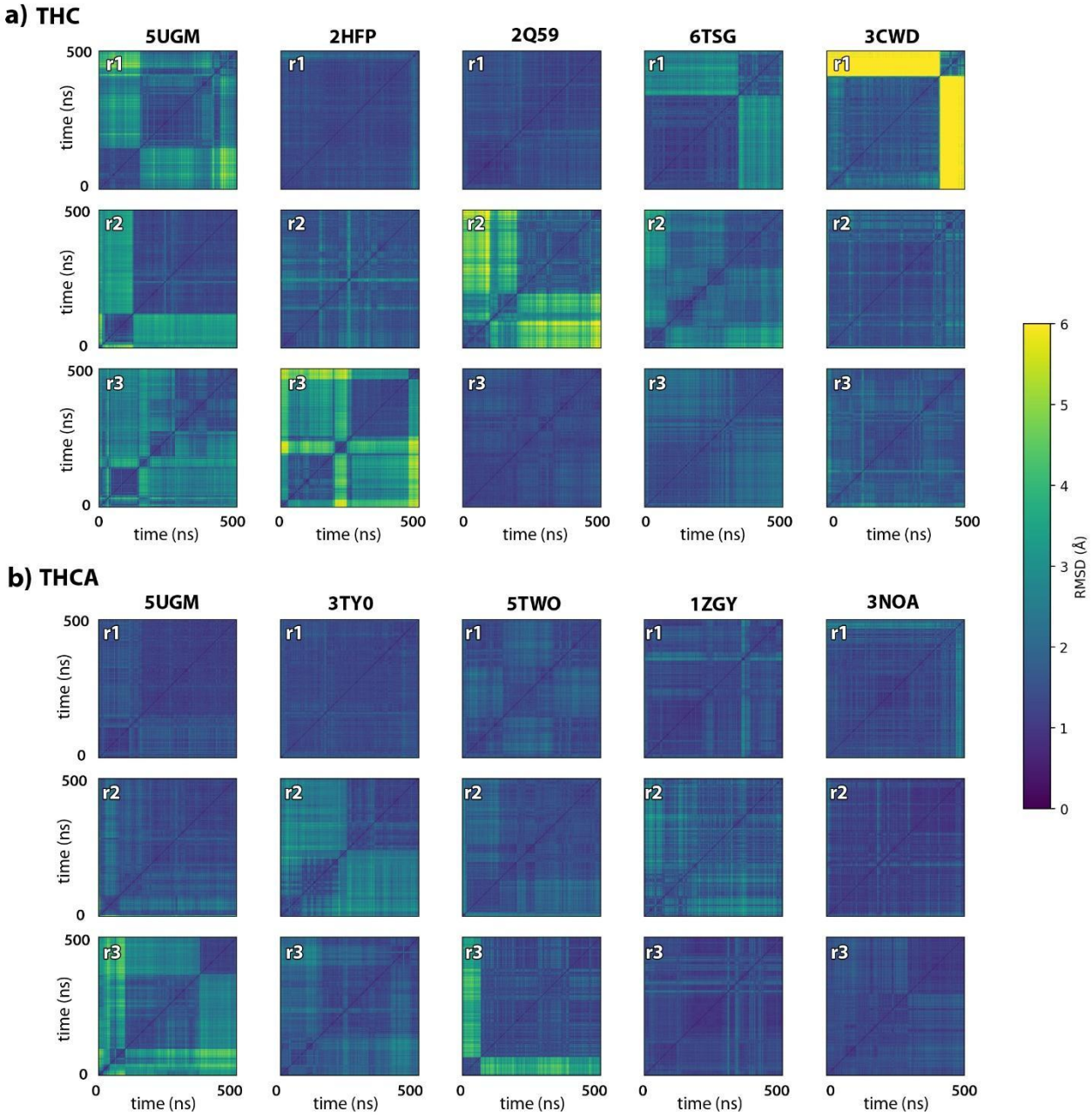


**Supplementary Figure S6.** Pairwise ligand RMSD computed for the THC (a) and THCA (b) systems.

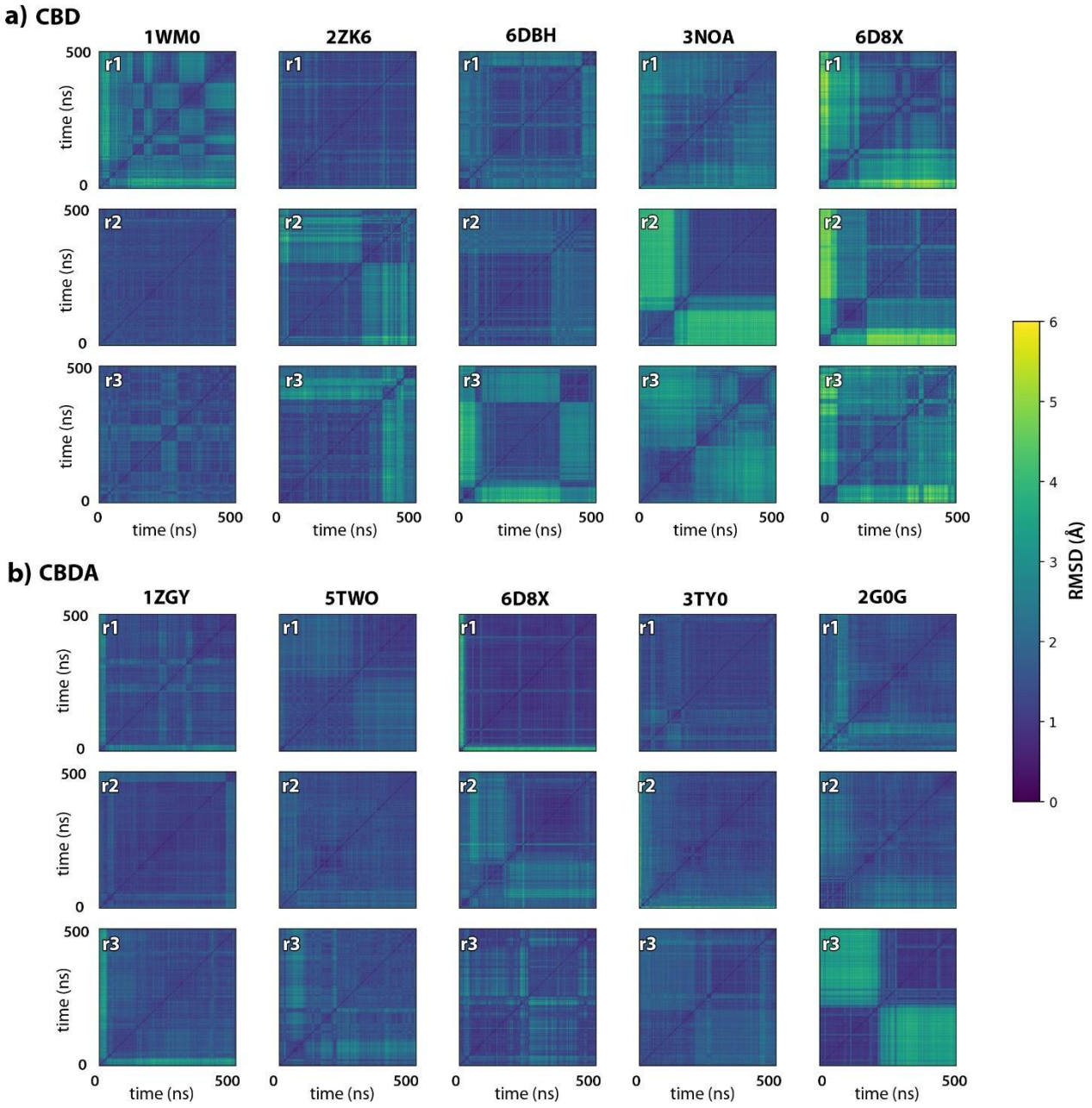


**Supplementary Figure S7.** Pairwise ligand RMSD computed for the CBD (a) and CBDA (b) systems.

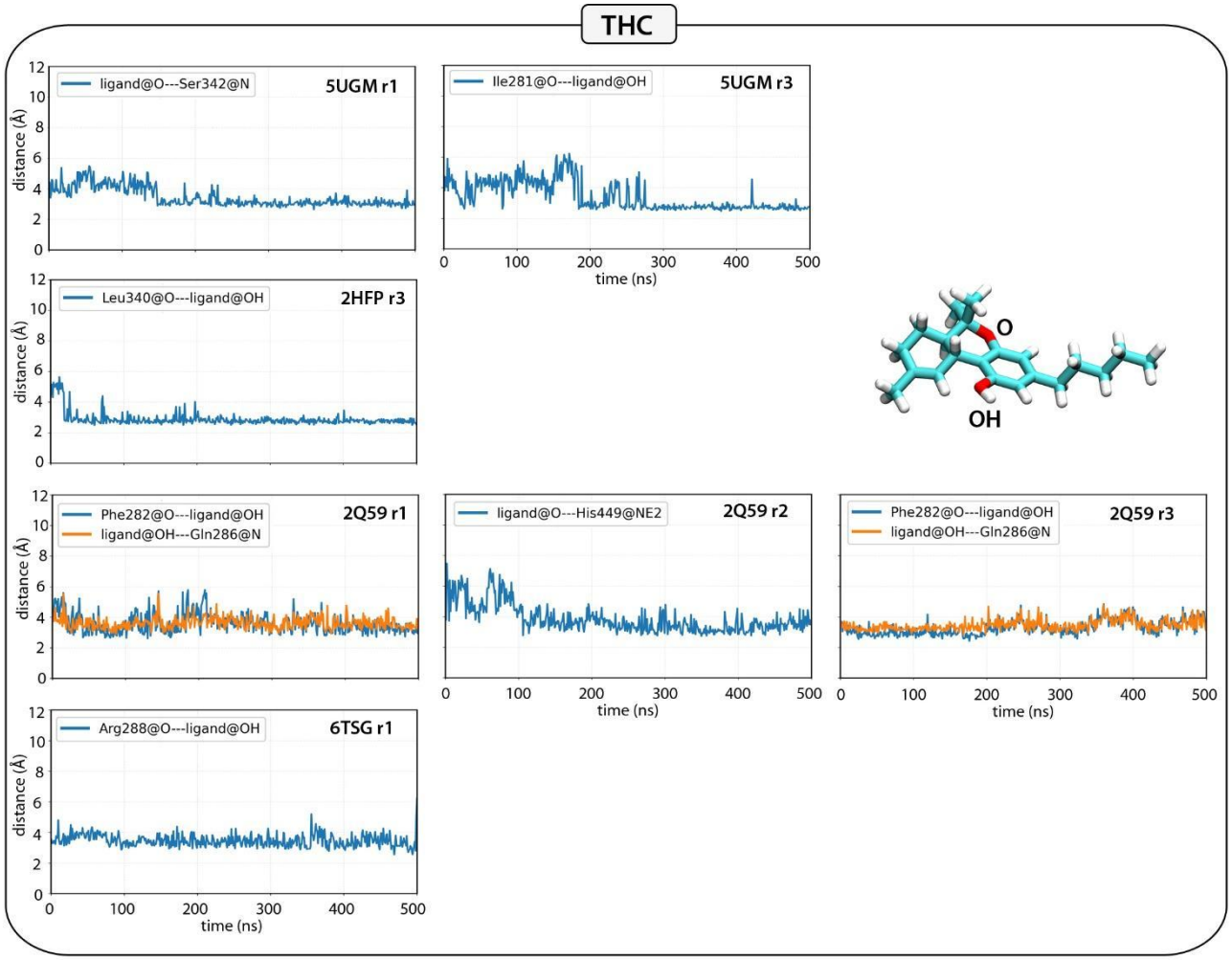


**Supplementary Figure S8.** Time evolution of the distances between PPARγ and THC atoms involved in the polar interaction identified along the simulations.

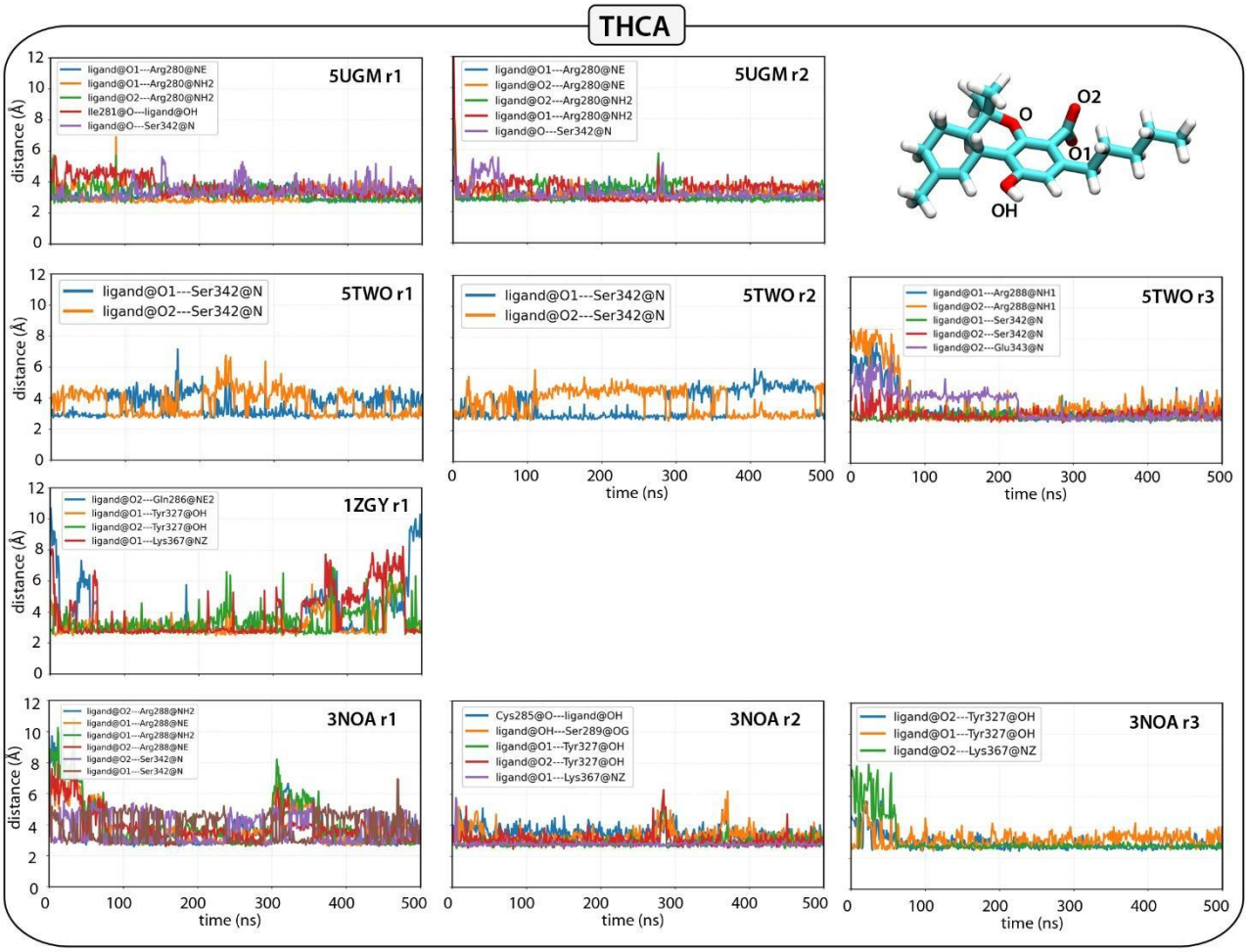


**Supplementary Figure S9.** Time evolution of the distances between PPARγ and THCA atoms involved in the polar interaction identified along the simulations.

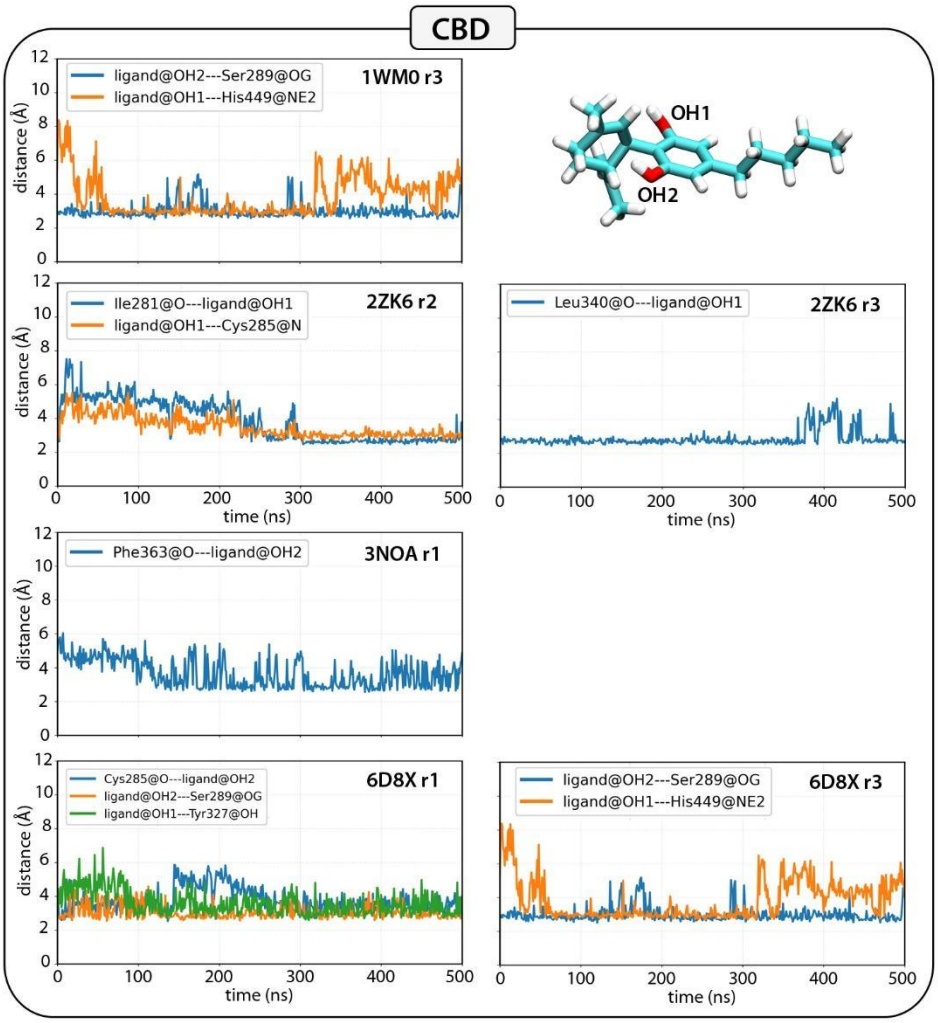


**Supplementary Figure S10.** Time evolution of the distances between PPARγ and CBD atoms involved in the polar interaction identified along the simulations.

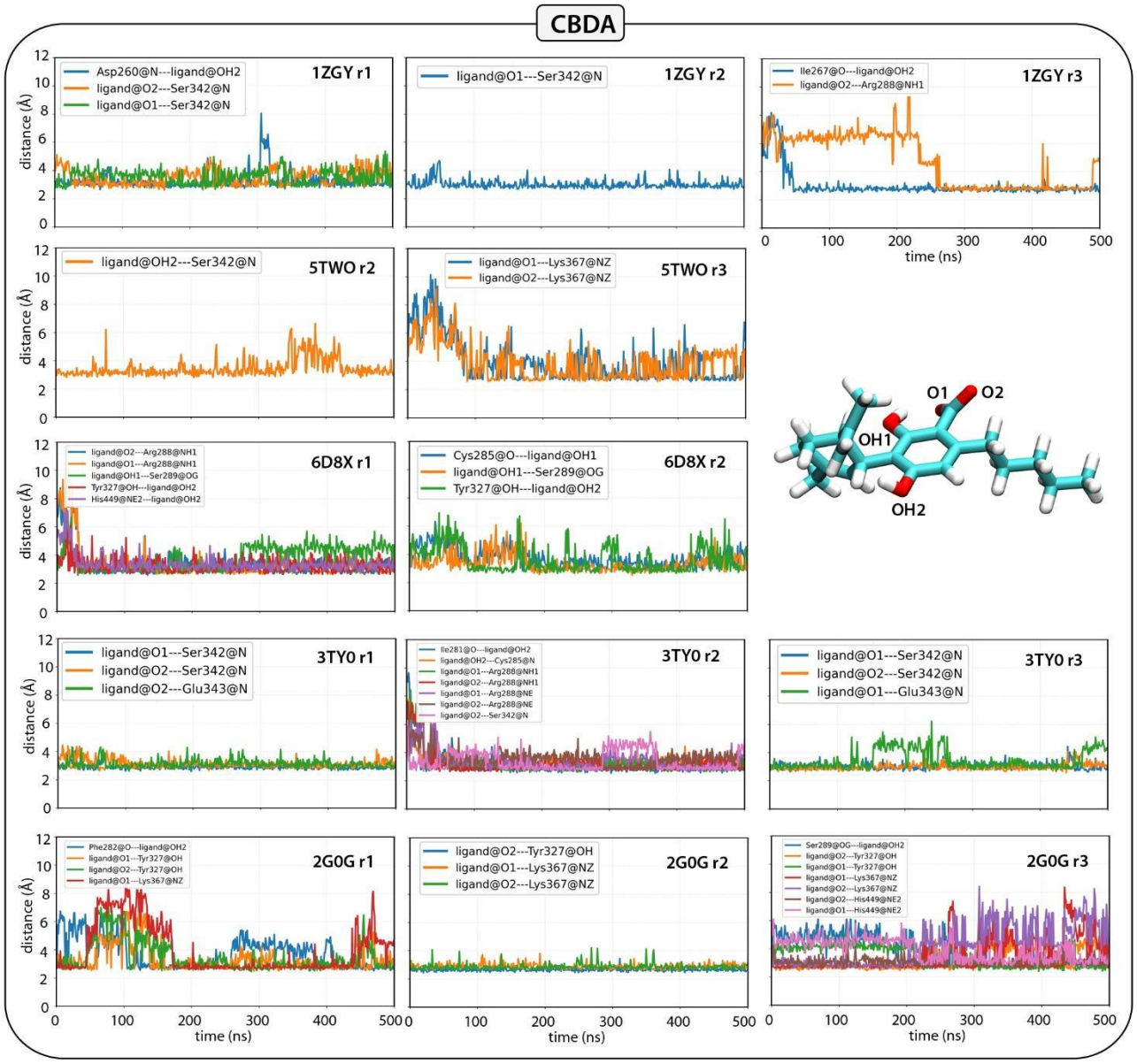


**Supplementary Figure S11.** Time evolution of the distances between PPARγ and CBDA atoms involved in the polar interaction identified along the simulations.

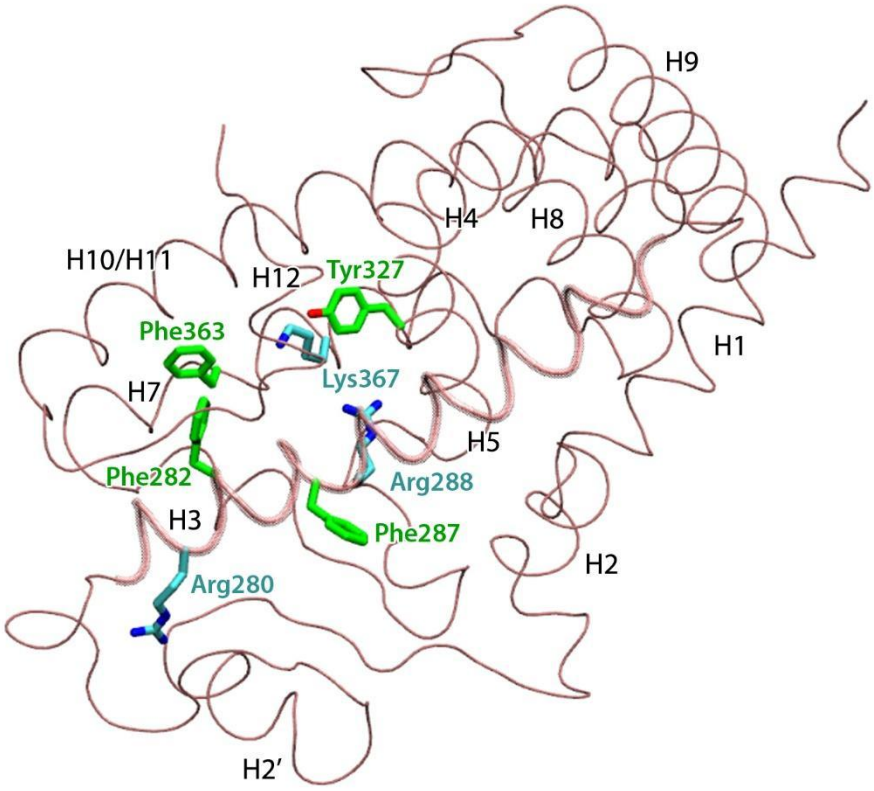


**Supplementary Figure S12.** Location of the basic residues (cyan carbons) and aromatic residues (green carbons) that interact with the cannabinoids in at least one of the MD simulations, shown on the PPARγ LBD-apo structure (PDB ID: 1PRG).

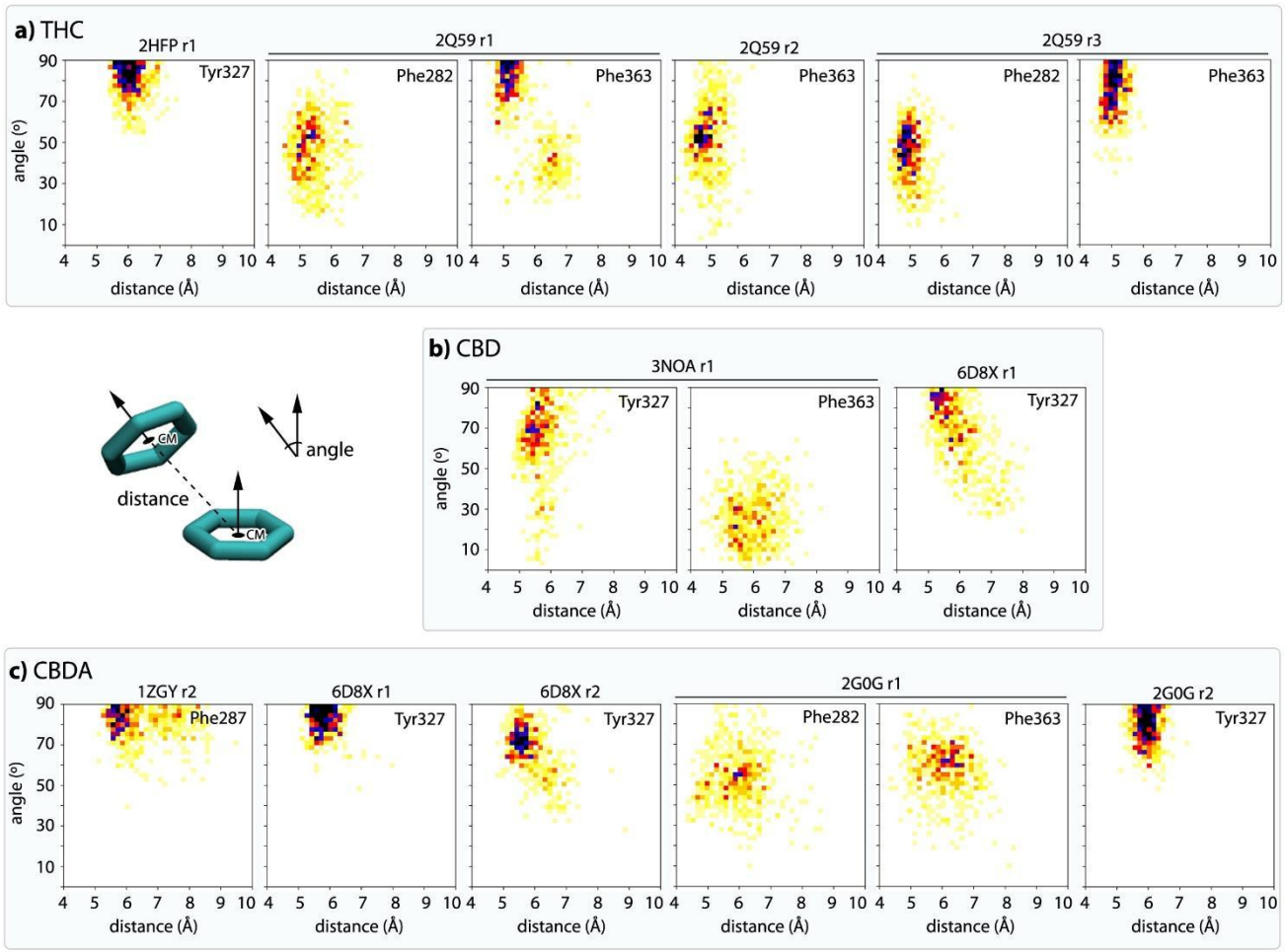


**Supplementary Figure S13.** 2D histograms showing the distribution of the distance between the centers of mass and the angle between the normal vectors of the cannabinoid resorcinol ring and the side chains of the indicated aromatic residues.

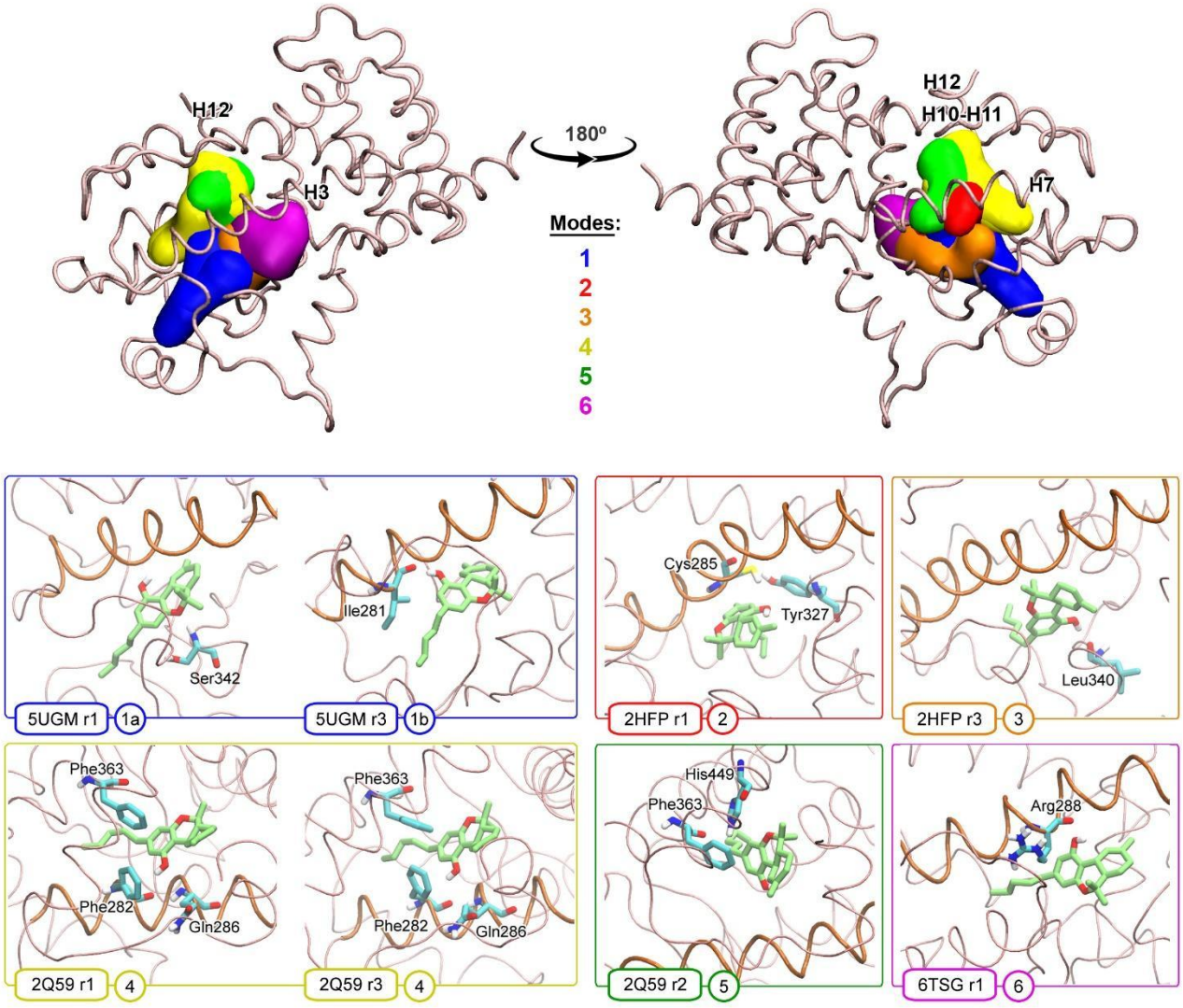


**Supplementary Figure S14.** Binding modes obtained for THC. Representative snapshots of each principal cluster of different MD simulations are shown. THC (carbons depicted in lime), contacting residues (carbons depicted in cyan), helix 3 is highlighted. PDB ID, replica, and number of binding mode are indicated for each snapshot. Similar binding modes are grouped together.

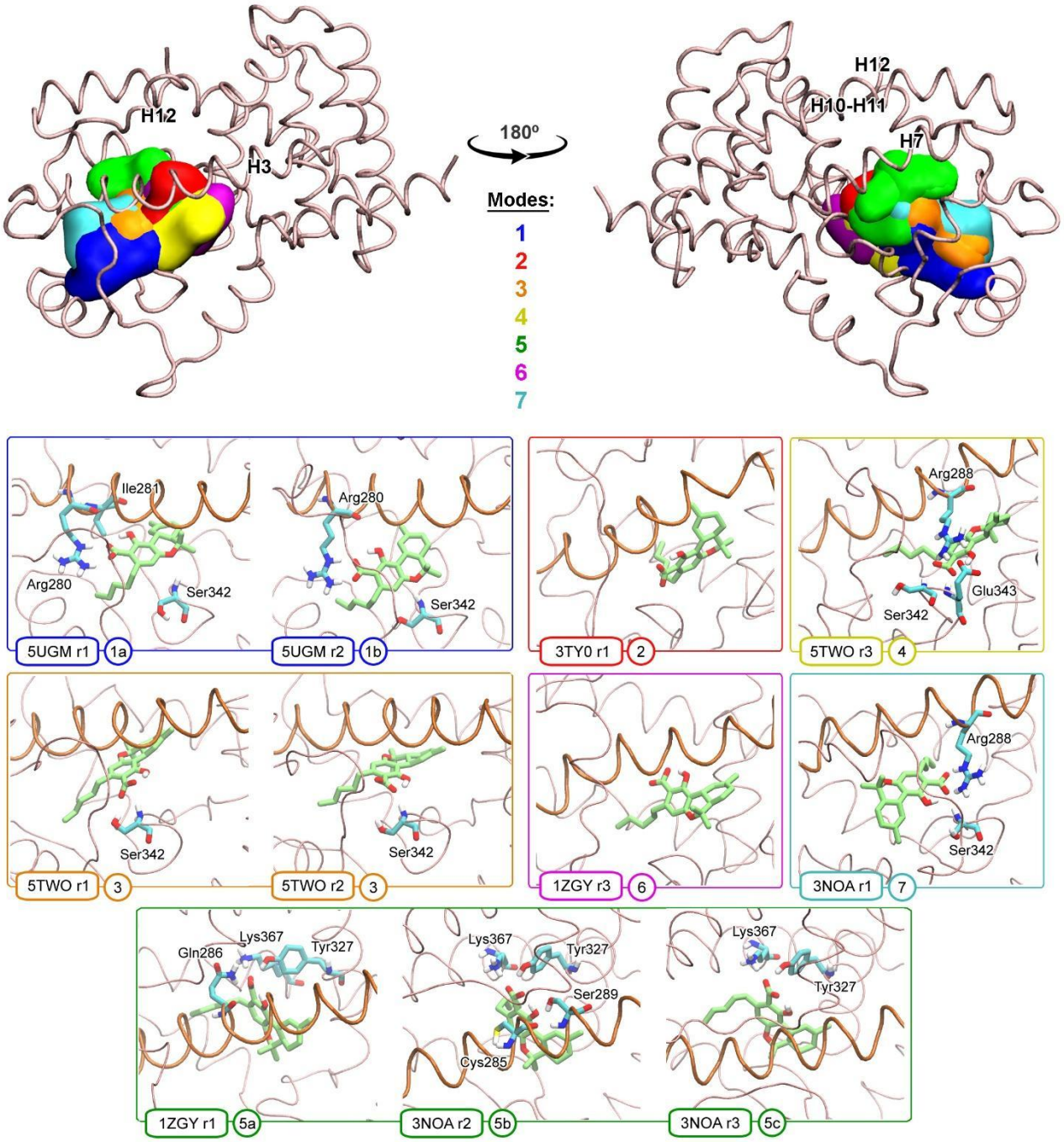


**Supplementary Figure S15.** Binding modes obtained for THCA. Representative snapshots of each principal cluster of different MD simulations are shown. THCA (carbons depicted in lime), contacting residues (carbons depicted in cyan), helix 3 is highlighted. PDB ID, replica, and number of binding mode for THCA are indicated for each snapshot. Similar binding modes are grouped together.

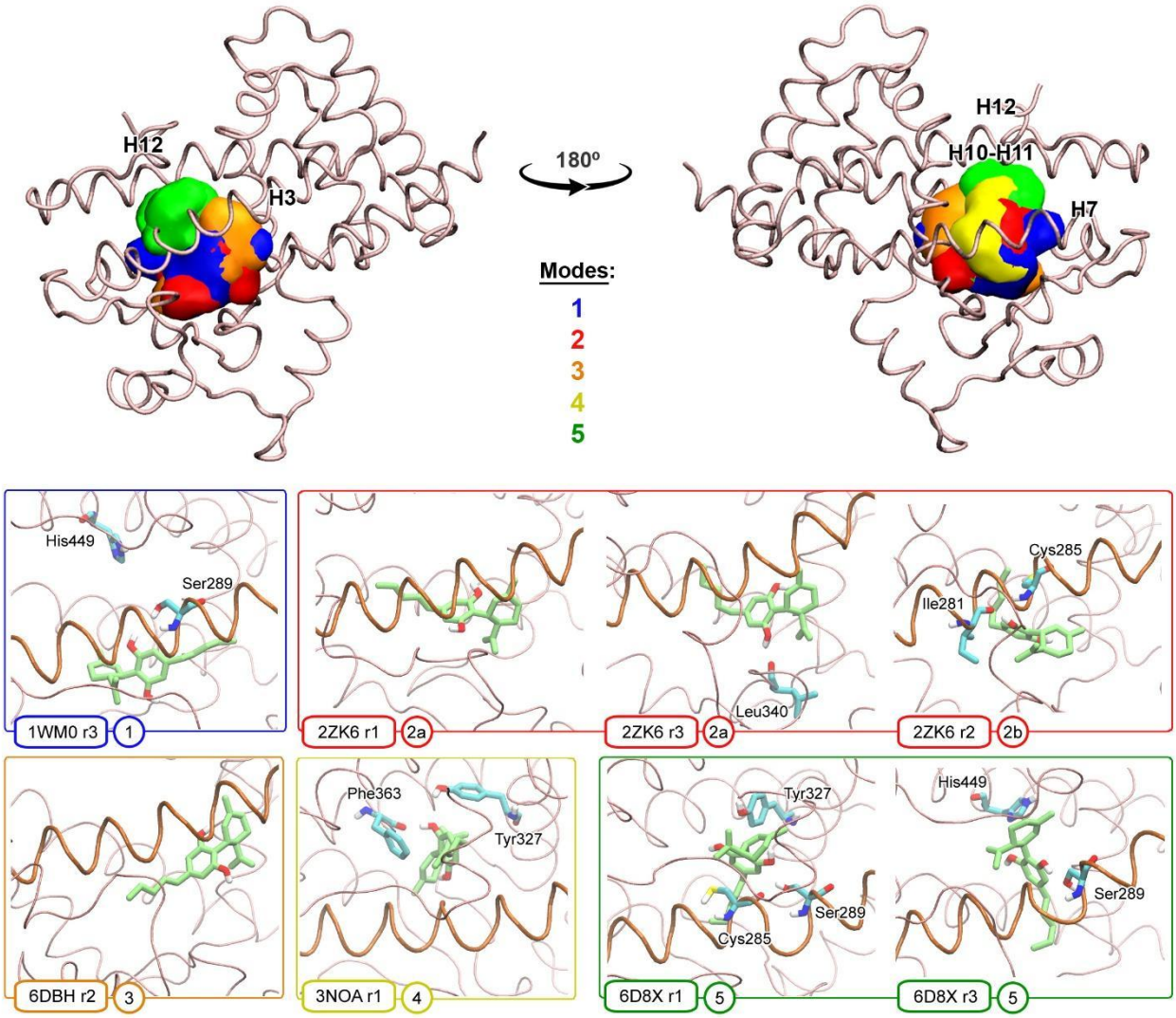


**Supplementary Figure S16.** Binding modes obtained for CBD. Representative snapshots of each principal cluster of different MD simulations are shown. CBD (carbons depicted in lime), contacting residues (carbons depicted in cyan), helix 3 is highlighted. PDB ID, replica, and number of binding mode for CBD are indicated for each snapshot. Similar binding modes are grouped together.

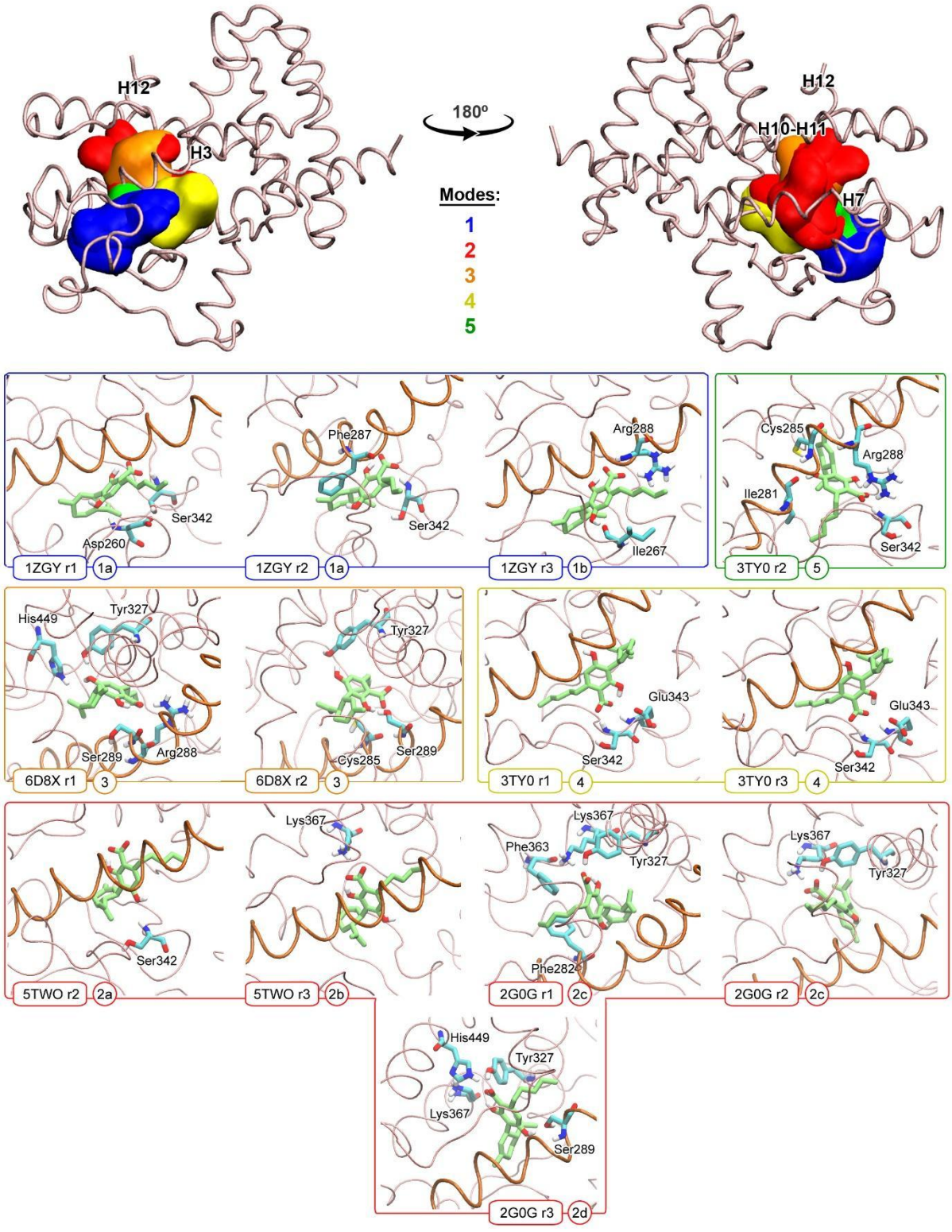


**Supplementary Figure S17.** Binding modes obtained for CBDA. Representative snapshots of each principal cluster of different MD simulations are shown. CBDA (carbons depicted in lime), contacting residues (carbons depicted in cyan), helix 3 is highlighted. PDB ID, replica, and number

of binding mode for CBDA are indicated for each snapshot. Similar binding modes are grouped together.

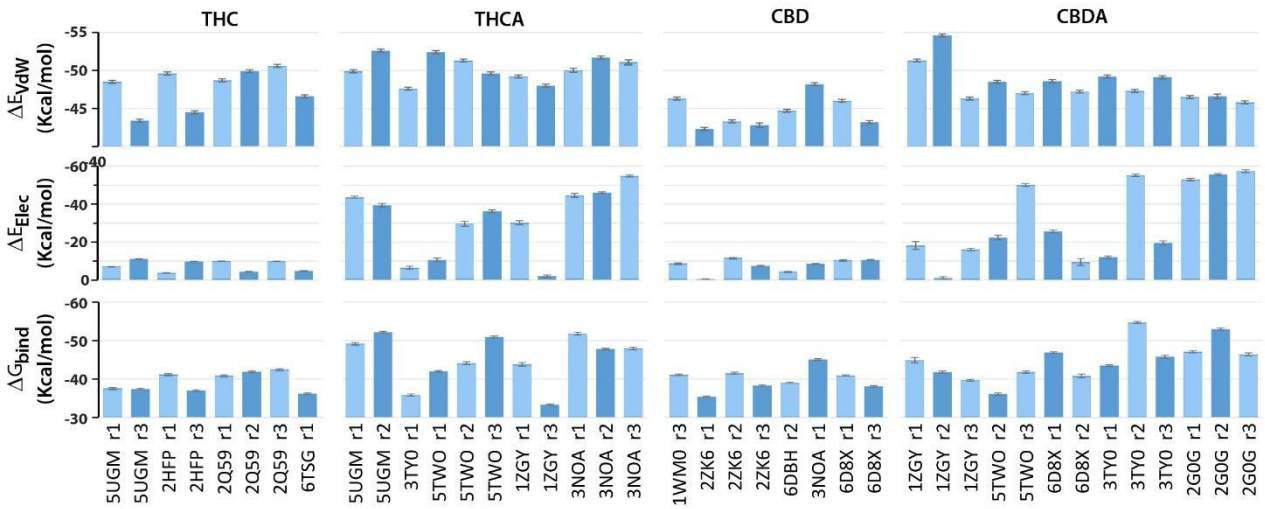


**Supplementary Figure S18.** MM/GBSA energy contributions for the selected systems.

| PDB ID | Chain | Res (Å) | Missing residues | PDB ID | Chain | Res (Å) | Missing residues |
|---|---|---|---|---|---|---|---|
| 1FM9 | B | 2.1 | - | 3TY0 | A | 2.0 | - |
| 1I7I | A | 2.4 | 267 to 275 | 3VJH | A | 2.2 | 262 to 274 |
| 1NYX | A | 2.7 | 262 to 276 | 3VN2 | A | 2.2 | 263 to 272 |
| 1WM0 | A | 2.9 | 268 to 273 | 3VSO | A | 2.0 | 265 to 273 |
| 1ZEO | A | 2.5 | 264 to 271 | 4A4W | A | 2.0 | 262 to 273 |
| 1ZGY | A | 1.8 | - | 4FGY | A | 2.8 | 290 to 294 |
| 2ATH | A | 2.3 | - | 4HEE | A | 2.5 | 241 to 243; 262 to 275 |
| 2FVJ | A | 2.0 | 262 to 274 | 4JAZ | A | 2.9 | - |
| 2G0G | A | 2.5 | - | 4PRG | A | 2.9 | - |
| 2HFP | A | 2.0 | - | 4PVU | A | 2.6 | 265 to 275 |
| 2I4Z | A | 2.3 | - | 4R06 | A | 2.2 | 239 to 240; 260 to 275 |
| 2OM9 | A | 2.8 | - | 5GTN | A | 1.9 | 269 to 273 |
| 2P4Y | A | 2.3 | 229 to 223; 255 to 278 | 5TWO | A | 1.9 | - |
| 2POB | A | 2.3 | 241 to 243; 264 to 274 | 5UGM | A | 2.1 | - |
| 2Q59 | A | 2.2 | 261 to 274; 285 | 6AD9 | A | 2.2 | 242; 262 to 274 |
| 2ZK5 | A | 2.5 | - | 6AUG | A | 2.7 | 264 to 275 |
| 2ZK6 | A | 2.4 | - | 6AVI | A | 2.3 | 263 to 274 |
| 2ZNO | A | 2.4 | 263 to 270 | 6D3E | A | 2.4 | 263 to 272 |
| 3ADS | A | 2.3 | 264 to 275 | 6D8X | A | 1.9 | - |
| 3BC5 | A | 2.3 | 242 to 244; 267 to 274 | 6DBH | A | 2.6 | - |
| 3CWD | A | 2.4 | 261 to 273 | 6DCU | A | 3.0 | 263 to 272 |
| 3ET3 | A | 2.0 | 263 to 274 | 6DGO | A | 3.1 | 267 to 274 |
| 3FUR | A | 2.3 | 259 to 274 | 6ENQ | A | 2.2 | 259 to 274 |
| 3G9E | A | 2.3 | 262 to 274 | 6IJS | A | 2.2 | 264 to 274 |
| 3H0A | B | 2.1 | 244 to 261 | 6IZN | A | 1.8 | 270 to 275 |
| 3HO0 | A | 2.6 | - | 6JF0 | A | 3.4 | 241; 264 to 274 |
| 3IA6 | A | 2.3 | 262 to 275 | 6K0T | A | 1.8 | 263 to 274; 285 |
| 3NOA | A | 2.0 | - | 6L89 | A | 2.1 | 264 to 274 |
| 3OSW | A | 2.6 | 263 to 273 | 6MD0 | A | 2.0 | 240 to 241; 264 to 274 |
| 3QT0 | A | 2.5 | 241 to 244 | 6MS7 | A | 1.4 | 265 to 271 |
| 3R5N | A | 2.0 | 242 to 243; 265 to 273 | 6TDC | A | 2.3 | 289 to 302 |
| 3R8A | A | 2.4 | 241 to 242; 263 to 273 | 6TSG | A | 3.0 | 261 to 275 |
| 3R8I | A | 2.3 | - | 6Y3U | A | 2.6 | 261 to 275 |
| 3S9S | A | 2.6 | 240 to 243; 269 to 274 | 6ZLY | A | 1.8 | 260 to 275 |
| 3T03 | A | 2.1 | 296 to 298 | 7AWD | A | 1.9 | 265 to 268 |

**Supplementary Table S1**. PPARγ crystal structures used for cannabinoid docking calculations.

| THC | | | | |
|---|---|---|---|---|
| **PDB ID** | **Lowest binding energy (Kcal/mol)** | **Mean binding energy (Kcal/mol)** | **Frequency (%)** | **Cluster** |
| 3IA6 | −10.5 | −9.9 | 63.8 | 1 |
| 5UGM | −11.6 | −10.9 | 60.7 | 1 |
| 1FM9 | −11.0 | −10.2 | 58.6 | 1 |
| 3ET3 | −11.1 | −10.3 | 53.0 | 1 |
| 2POB | −10.9 | −10.3 | 51.7 | 1 |
| 6AUG | −11.3 | −10.7 | 49.0 | 1 |
| 3BC5 | −10.8 | −10.3 | 46.4 | 1 |
| 3VSO | −10.2 | −9.7 | 43.4 | 1 |
| 3S9S | −11.5 | −10.6 | 39.8 | 1 |
| 1WM0 | −13.7 | −12.9 | 38.1 | 1 |
| 4JAZ | −11.1 | −10.5 | 37.6 | 1 |
| 3QT0 | −11.2 | −10.5 | 37.0 | 1 |
| 3G9E | −10.1 | −9.4 | 36.4 | 1 |
| 3R5N | −10.5 | −10.1 | 36.1 | 1 |
| 3NOA | −10.9 | −10.3 | 35.4 | 1 |
| 6IZN | −11.2 | −10.5 | 35.3 | 1 |
| 5TWO | −11.9 | −11.2 | 35.1 | 1 |
| 3ADS | −9.3 | −8.9 | 33.2 | 1 |
| 6ENQ | −9.9 | −9.3 | 33.0 | 1 |
| 5GTN | −12.1 | −11.3 | 32.1 | 1 |
| 1NYX | −11.0 | −10.0 | 64.3 | 2 |
| 4R06 | −10.5 | −9.9 | 48.4 | 2 |
| 2HFP | −11.3 | −10.3 | 47.1 | 2 |
| 3H0A | −10.8 | −10.0 | 42.2 | 2 |
| 1I7I | −10.1 | −9.6 | 40.0 | 2 |
| 4FGY | −10.2 | −9.2 | 39.7 | 2 |
| 6MD0 | −10.0 | −9.5 | 37.5 | 2 |
| 6AD9 | −9.9 | −9.4 | 36.9 | 2 |
| 3T03 | −10.2 | −9.5 | 36.8 | 2 |
| 6ZLY | −10.4 | −9.8 | 35.5 | 2 |
| 6AVI | −10.6 | −10.0 | 34.8 | 2 |
| 6AVI | −11.0 | −10.3 | 33.7 | 2 |
| 6DCU | −10.4 | −9.7 | 31.5 | 2 |
| 1ZGY | −10.3 | −9.5 | 30.4 | 2 |
| 2Q59 | −11.3 | −10.1 | 41.6 | 3 |
| 6TSG | −10.3 | −9.5 | 30.2 | 4 |
| 3CWD | −9.2 | −8.7 | 33.0 | 5 |

**Supplementary Table S2a**. Docking results for THC in PPARγ.

| THCA | | | | |
|---|---|---|---|---|
| **PDB ID** | **Lowest binding energy (Kcal/mol)** | **Mean binding energy (Kcal/mol)** | **Frequency (%)** | **Cluster** |
| 3IA6 | −10.5 | −9.8 | 69.4 | 1 |
| 3ADS | −9.6 | −8.9 | 62.6 | 1 |
| 6AVI | −10.7 | −9.9 | 62.3 | 1 |
| 5UGM | −11.7 | −10.9 | 58.2 | 1 |
| 4A4W | −9.8 | −9.0 | 55.7 | 1 |
| 3G9E | −10.1 | −9.3 | 55.1 | 1 |
| 1FM9 | −11.1 | −10.3 | 54.9 | 1 |
| 3VSO | −10.4 | −9.9 | 48.5 | 1 |
| 6IZN | −11.4 | −10.3 | 46.5 | 1 |
| 1I7I | −10.4 | −9.5 | 46.4 | 1 |
| 6DCU | −10.2 | −9.2 | 46.1 | 1 |
| 3ET3 | −11.4 | −10.3 | 43.9 | 1 |
| 6MD0 | −10.2 | −9.5 | 43.4 | 1 |
| 6JF0 | −10.4 | −9.5 | 42.6 | 1 |
| 4R06 | −10.6 | −9.8 | 41.5 | 1 |
| 3BC5 | −10.9 | −10.3 | 40.4 | 1 |
| 6ENQ | −10.2 | −9.4 | 38.4 | 1 |
| 1NYX | −10.4 | −9.6 | 37.8 | 1 |
| 6Y3U | −9.0 | −8.0 | 37.0 | 1 |
| 3R8I | −10.9 | −10.0 | 33.6 | 1 |
| 2ATH | −10.4 | −9.8 | 32.5 | 1 |
| 1NYX | −10.1 | −9.3 | 32.1 | 1 |
| 4JAZ | −11.4 | −10.5 | 31.6 | 1 |
| 3VN2 | −9.9 | −9.0 | 31.1 | 1 |
| 4HEE | −9.5 | −8.8 | 30.7 | 1 |
| 4PVU | −9.5 | −8.8 | 30.7 | 1 |
| 6TSG | −10.5 | −9.5 | 52.5 | 2 |
| 3TY0 | −10.8 | −10.0 | 35.2 | 2 |
| 5TWO | −12.1 | −10.9 | 39.2 | 3 |
| 3S9S | −11.8 | −10.6 | 34.2 | 3 |
| 1ZGY | −10.0 | −9.1 | 49.4 | 4 |
| 3NOA | −11.0 | −10.1 | 32.8 | 5 |

**Supplementary Table S2b**. Docking results for THCA in PPARγ.

| CBD | | | | |
|---|---|---|---|---|
| **PDB ID** | **Lowest binding energy (Kcal/mol)** | **Mean binding energy (Kcal/mol)** | **Frequency (%)** | **Cluster** |
| 1WM0 | −10.9 | −9.1 | 29.9 | 1 |
| 4HEE | −10.5 | −9.3 | 29.4 | 1 |
| 6DGO | −10.3 | −8.9 | 20.0 | 1 |
| 6IZN | −10.3 | −8.8 | 18.0 | 1 |
| 3S9S | −11.7 | −9.9 | 17.0 | 1 |
| 3S9S | −10.6 | −9.3 | 16.3 | 1 |
| 1NYX | −10.1 | −9.0 | 19.8 | 2 |
| 2ZK6 | −11.0 | −9.3 | 17.6 | 2 |
| 6ZLY | −10.9 | −9.0 | 17.6 | 2 |
| 6L89 | −10.4 | −9.0 | 16.6 | 2 |
| 3CWD | −8.7 | −8.1 | 15.7 | 2 |
| 2P4Y | −9.0 | −8.1 | 15.6 | 3 |
| 6DBH | −11.3 | −10.1 | 15.5 | 3 |
| 6MS7 | −10.6 | −9.2 | 15.1 | 3 |
| 3NOA | −10.3 | −9.5 | 17.0 | 4 |
| 2HFP | −11.0 | −9.3 | 15.6 | 4 |
| 6D8X | −10.5 | −9.2 | 19.3 | 5 |
| 2POB | −10.8 | −9.5 | 15.6 | 5 |

**Supplementary Table S2c**. Docking results for CBD in PPARγ.

| CBDA | | | | |
|---|---|---|---|---|
| **PDB ID** | **Lowest binding energy (Kcal/mol)** | **Mean binding energy (Kcal/mol)** | **Frequency (%)** | **Cluster** |
| 1FM9 | −10.2 | −8.5 | 17.2 | 1 |
| 1ZGY | −9.4 | −8.2 | 21.8 | 1 |
| 2FVJ | −9.5 | −7.9 | 17.8 | 1 |
| 2POB | −10.2 | −8.6 | 15.9 | 1 |
| 3ADS | −9.0 | −7.8 | 21.2 | 1 |
| 3G9E | −9.1 | −7.8 | 17.6 | 1 |
| 3IA6 | −9.3 | −7.9 | 25.7 | 1 |
| 3VJH | −9.1 | −7.7 | 15.7 | 1 |
| 4HEE | −8.5 | −7.2 | 19.1 | 1 |
| 4PVU | −9.1 | −7.7 | 15.6 | 1 |
| 6AVI | −9.5 | −8.1 | 22.1 | 1 |
| 6DCU | −9.7 | −8.5 | 20.4 | 1 |
| 6TSG | −8.9 | −7.2 | 24.8 | 1 |
| 6Y3U | −8.1 | −7.0 | 24.6 | 1 |
| 1WM0 | −10.3 | −8.5 | 26.9 | 2 |
| 3QT0 | −9.3 | −8.1 | 20.2 | 2 |
| 3R8A | −9.0 | −7.6 | 18.3 | 2 |
| 3S9S | −10.7 | −9.2 | 19.5 | 2 |
| 5TWO | −10.4 | −8.8 | 23.0 | 2 |
| 6DBH | −10.5 | −8.6 | 17.6 | 2 |
| 1NYX | −10.3 | −9.3 | 18.5 | 3 |
| 1ZEO | −9.8 | −8.5 | 21.3 | 3 |
| 6D8X | −9.9 | −8.5 | 19.3 | 3 |
| 1WM0 | −10.9 | −9.2 | 22.0 | 4 |
| 3CWD | −8.7 | −8.0 | 22.9 | 4 |
| 3TY0 | −10.8 | −9.8 | 15.8 | 4 |
| 2G0G | −10.7 | −8.6 | 24.0 | 5 |

**Supplementary Table S2d**. Docking results for CBDA in PPARγ.

| Receptor | Ligand | Run | Polar interaction | Aromatic-aromatic interaction | Binding Mode | Freq (%) |
|---|---|---|---|---|---|---|
| 5UGM | THC | 1 | Ser342 | - | 1a | 98 |
| 5UGM | THC | 3 | Ile281 | - | 1b | 96 |
| 2HFP | THC | 1 | - | Tyr327 | 2 | 94 |
| 2HFP | THC | 3 | Leu340 | - | 3 | 84 |
| 2Q59 | THC | 1 | Phe282, Gln286 | Phe282, Phe363 | 4 | 89 |
| 2Q59 | THC | 2 | His449 | Phe363 | 5 | 92 |
| 2Q59 | THC | 3 | Phe282, Gln286 | Phe282, Phe363 | 4 | 92 |
| 6TSG | THC | 1 | Arg288 | - | 6 | 78 |
| 5UGM | THCA | 1 | Arg280, Ile281, Ser342 | - | 1a | 99 |
| 5UGM | THCA | 2 | Arg280, Ser342 | - | 1b | 94 |
| 3TY0 | THCA | 1 | - | - | 2 | 92 |
| 5TWO | THCA | 1 | Ser342 | - | 3 | 96 |
| 5TWO | THCA | 2 | Ser342 | - | 3 | 91 |
| 5TWO | THCA | 3 | Arg288, Ser342, Glu343 | - | 4 | 98 |
| 1ZGY | THCA | 1 | Gln286, Tyr327, Lys367 | - | 5a | 93 |
| 1ZGY | THCA | 3 | - | - | 6 | 91 |
| 3NOA | THCA | 1 | Arg288, Ser342 | - | 7 | 81 |
| 3NOA | THCA | 2 | Cys285, Ser289, Tyr327, Lys367 | - | 5b | 98 |
| 3NOA | THCA | 3 | Tyr327, Lys367 | - | 5c | 97 |
| 1WM0 | CBD | 3 | Ser289, His449 | - | 1 | 92 |
| 2ZK6 | CBD | 1 | - | - | 2a | 97 |
| 2ZK6 | CBD | 2 | Ile281, Cys285 | - | 2b | 86 |
| 2ZK6 | CBD | 3 | Leu340 | - | 2a | 98 |
| 6DBH | CBD | 2 | - | - | 3 | 92 |
| 3NOA | CBD | 1 | Phe363 | Tyr327, Phe363 | 4 | 94 |
| 6D8X | CBD | 1 | Cys285, Ser289, Tyr327 | Tyr327 | 5 | 86 |
| 6D8X | CBD | 3 | Ser289, His449 | - | 5 | 93 |
| 1ZGY | CBDA | 1 | Asp260, Ser342 | - | 1a | 97 |
| 1ZGY | CBDA | 2 | Ser342 | Phe287 | 1a | 85 |
| 1ZGY | CBDA | 3 | Ile267, Arg288 | - | 1b | 97 |
| 5TWO | CBDA | 2 | Ser342 | - | 2a | 98 |
| 5TWO | CBDA | 3 | Lys367 | - | 2b | 93 |
| 6D8X | CBDA | 1 | Arg288, Ser289, Tyr327, His449 | Tyr327 | 3 | 97 |
| 6D8X | CBDA | 2 | Cys285, Ser289, Tyr327 | Tyr327 | 3 | 95 |
| 3TY0 | CBDA | 1 | Ser342, Glu343 | - | 4 | 96 |
| 3TY0 | CBDA | 2 | Ile281, Cys285, Arg288, Ser342 | - | 5 | 97 |
| 3TY0 | CBDA | 3 | Ser342, Glu343 | - | 4 | 93 |

| | | | | | | |
|---|---|---|---|---|---|---|
| 2G0G | CBDA | 1 | Phe282, Tyr327, Lys367 | Phe282, Phe363 | 2c | 94 |
| 2G0G | CBDA | 2 | Tyr327, Lys367 | Tyr327 | 2c | 86 |
| 2G0G | CBDA | 3 | Ser289, Tyr327, Lys367, His449 | - | 2d | 93 |

**Supplementary Table S3**. Subset of MD systems selected for the analysis. For each system, the residues involved in polar and aromatic-aromatic interactions with the cannabinoid are indicated, along with the assigned binding mode and the frequency of the corresponding representative cluster.

| Ligand | Receptor | Run | Mode | Resid | | | | | | | |
|---|---|---|---|---|---|---|---|---|---|---|---|
| | | | | Ser342 | | | | | | | |
| | | | | HBO | Ene | | | | | | |
| THC | 5UGM | r1 | 1a | 82 | −1.2 ± 0.5 | | | | | | |
| | | | | Phe282 | | Gln286 | | | | | |
| | | | | HBO | Ene | HBO | Ene | | | | |
| THC | 2Q59 | r3 | 4 | 67 | −3.1 ± 0.7 | 59 | −1.0 ± 0.4 | | | | |
| | | | | Arg280 | | Ile281 | | Ser342 | | | |
| | | | | HBO | Ene | HBO | Ene | HBO | Ene | | |
| THCA | 5UGM | r1 | 1a | 90 | −9.0 ± 0.8 | 66 | −1.4 ± 0.2 | 51 | −1.0 ± 0.4 | | |
| | | | | Arg288 | | Ser342 | | Glu343 | | | |
| | | | | HBO | Ene | HBO | Ene | HBO | Ene | | |
| THCA | 5TWO | r3 | 4 | 62 | −9.0 ± 0.8 | 97 | −1.1 ± 0.4 | 56 | 0.4 ± 0.2 | | |
| | | | | Cys285 | | Ser289 | | Tyr327 | | Lys367 | |
| | | | | HBO | Ene | HBO | Ene | HBO | Ene | HBO | Ene |
| THCA | 3NOA | r2 | 5b | 55 | −2.7 ± 0.4 | 66 | −0.3 ± 0.2 | 89 | −1.9 ± 0.6 | 98 | −8.8 ± 1.5 |
| | | | | Ile281 | | Cys285 | | | | | |
| | | | | HBO | Ene | HBO | Ene | | | | |
| CBD | 2ZK6 | r2 | 2b | 52 | −2.1 ± 1.0 | 49 | −2.3 ± 0.7 | | | | |
| | | | | Cys285 | | Ser289 | | Tyr327 | | | |
| | | | | HBO | Ene | HBO | Ene | HBO | Ene | | |
| CBD | 6D8X | r1 | 5 | 46 | −1.8 ± 0.4 | 81 | −1.0 ± 0.8 | 44 | −0.8 ± 0.4 | | |
| | | | | Arg288 | | Ser289 | | Tyr327 | | His449 | |
| | | | | HBO | Ene | HBO | Ene | HBO | Ene | HBO | Ene |
| CBDA | 6D8X | r1 | 3 | 85 | −8.0 ± 0.8 | 67 | −0.6 ± 0.5 | 76 | −0.8 ± 0.5 | 80 | −0.9 ± 0.6 |
| | | | | Ile281 | | Cys285 | | Arg288 | | Ser342 | |
| | | | | HBO | Ene | HBO | Ene | HBO | Ene | HBO | Ene |
| CBDA | 3TY0 | r2 | 5 | 90 | −4.0 ± 0.9 | 68 | −1.9 ± 0.6 | 78 | −7.4 ± 2.5 | 51 | −2.6 ± 0.9 |
| | | | | Tyr327 | | Lys367 | | | | | |
| | | | | HBO | Ene | HBO | Ene | | | | |
| CBDA | 2G0G | r2 | 2c | 99 | −3.6 ± 0.7 | 98 | −11.3 ± 1.7 | | | | |

**Supplementary Table S4**. Hydrogen-bond occupancies (HBO, %) and per-residue MM/GBSA decomposition energies (Ene, Kcal/mol) for residues participating in polar interactions with the ligands in the different PPARγ/cannabinoid systems.